Supporting Information: Systematic over-estimation of lattice thermal conductivity in materials with electrically-resistive grain boundaries

Jimmy Jiahong Kuo, Max Wood, Tyler J. Slade, Mercouri G. Kanatzidis, and G. Jeffrey Snyder*

Northwestern University, Evanston, IL 60208, USA

E-mail: jeff.snyder@northwestern.edu

S1 Bulk conductivity

In this paper, the weighted mobility μ_w of large-grain (>30 μm) n-type $Mg_3Sb_{1.5}Bi_{0.5}$, previously reported[1] with an approximately $T^{-3/2}$ trend, is considered as the weighted mobility of the bulk $\mu_{\text{w, bulk}}$. Given a known Seebeck coefficient of a sample, the Fermi level can be calculated (using Eq. (11.2) in Ref. 2). Using the bulk weighted mobility and the Fermi level, the bulk conductivity can be calculated (using Eq. (42) and (49) in Ref. 3), which is shown as the black solid line in Fig.3 in the main text.

In this manuscript, the μ_w in Fig. 1 and Fig. 6 are the total μ_w calculated using measured conductivity and Seebeck coefficient. When resistive grain boundaries exist in a sample, the total μ_w will be smaller than in a single crystal sample. For example, grain-boundary resistance often dominates near room temperature, and becomes less significant as the temperature increases. In large-grain samples, μ_w typically show a $T^{-3/2}$ trend, while in small-grain samples μ_w is usually smaller at low temperature and gradually converges to μ_w of the large-grain samples at high temperature. As a result, a comparison of μ_w between samples with different grain sizes at different temperatures can be a first-order method to characterize grain-boundary effect on charge transport.

S2 The thin grain-boundary approximation

In the series-circuit model, the heat conduction is determined by the thermal resistance of the bulk grains and that of the grain boundaries. The width of the grain-boundary resistor is relatively thin compared to that of the bulk ($\ell_\mathrm{GB}/\ell_\mathrm{G} \approx 10^{-3}$ in Mg_3Sb_2[4]). As a result, for the grain-boundary thermal resistance to be significant the ratio between their thermal conductivities κ_{GB}/κ_G has to be in the same order of magnitude as $\ell_\mathrm{GB}/\ell_\mathrm{G}$ which is unlikely given the low thermal conductivity of Mg_3Sb_2 which is within a factor of 10 of the minimum thermal conductivity estimated from a diffusion model.[5] This is in contrast to charge transport, where a small ratio of electrical conductivity $\sigma_\mathrm{GB}/\sigma_\mathrm{G}$ can be easily achieved via a low local carrier concentration.

S3 Annealing effect on Seebeck

Fig. S1 shows the Seebeck coefficient before and after annealing in Mg vapor. Before annealing, the Seebeck coefficient is positive and decrease with temperature, which means the majority charge carrier is holes (p-type) and the transport is similar to intrinsic semiconductors. After annealing, the Seebeck coefficient becomes negative (n-type) and the absolute value increases with temperature, which is the typically behavior of heavily doped semiconductors and is consistent with literature data of Mg_3Sb_2.

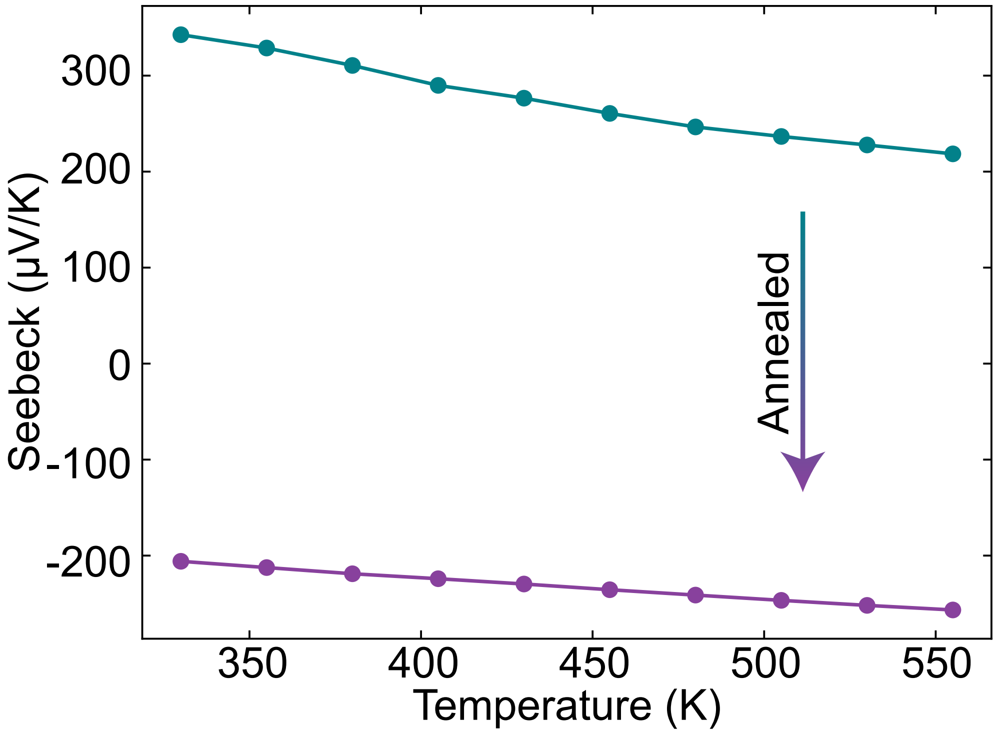

Figure S1: Temperature dependence of Seebeck coefficient of Te-doped Mg_3Sb_2 (nominal composition: $Mg_{3\text{-}\delta}Sb_{1.5}Bi_{0.49}Te_{0.01}$) before (cyan color) and after (purple color) annealed in Mg vapor.

S4 Transport data of other systems

References

(1) Wood, M.; Kuo, J. J.; Imasato, K.; Snyder, G. J. Improvement of Low-Temperature zT in a Mg_3Sb_2–Mg_3Bi_2 Solid Solution via Mg-Vapor Annealing. *Advanced Materials* **2019**, 1902337.

(2) May, A. F.; Snyder, G. J. *Materials, preparation, and characterization in thermoelectrics*; CRC Press, 2017; pp 11–1.

(3) Zevalkink, A. et al. A practical field guide to thermoelectrics: Fundamentals, synthesis, and characterization. *Applied Physics Reviews* **2018**, *5*, 021303.

(4) Kuo, J. J.; Yu, Y.; Kang, S. D.; Cojocaru-Mirédin, O.; Wuttig, M.; Snyder, G. J. Mg

Deficiency in Grain Boundaries of n-Type Mg_3Sb_2 Identified by Atom Probe Tomography. *Advanced Materials Interfaces* **2019**, 1900429.

(5) Agne, M. T.; Hanus, R.; Snyder, G. J. Minimum thermal conductivity in the context of diffuson-mediated thermal transport. *Energy & Environmental Science* **2018**, *11*, 609–616.

(6) de Boor, J.; Dasgupta, T.; Kolb, H.; Compere, C.; Kelm, K.; Mueller, E. Microstructural effects on thermoelectric efficiency: A case study on magnesium silicide. *Acta Materialia* **2014**, *77*, 68–75.

(7) Slade, T. J.; Bailey, T. P.; Grovogui, J. A.; Hua, X.; Zhang, X.; Kuo, J. J.; Hadar, I.; Snyder, G. J.; Wolverton, C.; Dravid, V. P.; Uher, C.; Kanatzidis, M. G. High Thermoelectric Performance in PbSe–$NaSbSe_2$ Alloys from Valence Band Convergence and Low Thermal Conductivity. *Advanced Energy Materials* **2019**, 1901377.

(8) Slade, T. J.; Grovogui, J. A.; Kuo, J. J.; Anad, S.; Bailey, T. P.; Wood, M.; Uher, C.; Snyder, G. J.; Dravid, V. P.; Kanatzidis, M. G. *in Preparation* **2019**,

(9) Zhao, L.-D.; Lo, S.-H.; Zhang, Y.; Sun, H.; Tan, G.; Uher, C.; Wolverton, C.; Dravid, V. P.; Kanatzidis, M. G. Ultralow thermal conductivity and high thermoelectric figure of merit in SnSe crystals. *Nature* **2014**, *508*, 373.

(10) Lee, Y. K.; Luo, Z.; Cho, S. P.; Kanatzidis, M. G.; Chung, I. Surface oxide removal for polycrystalline SnSe reveals near-single-crystal thermoelectric performance. *Joule* **2019**, *3*, 719–731.

(11) Qiu, Q.; Liu, Y.; Xia, K.; Fang, T.; Yu, J.; Zhao, X.; Zhu, T. Grain Boundary Scattering of Charge Transport in n-Type (Hf, Zr) CoSb Half-Heusler Thermoelectric Materials. *Advanced Energy Materials* **2019**, *9*, 1803447.

(12) Zhou, Z.; Agne, M. T.; Zhang, Q.; Wan, S.; Song, Q.; Xu, Q.; Lu, X.; Gu, S.; Fan, Y.; Jiang, W.; Snyder, G. J.; Wang, L. Microstructure and composition engineering Yb single-filled CoSb3 for high thermoelectric and mechanical performances. *Journal of Materiomics* **2019**,

(13) Hu, L.; Liu, X.; Xie, H.; Shen, J.; Zhu, T.; Zhao, X. Improving thermoelectric properties of n-type bismuth–telluride-based alloys by deformation-induced lattice defects and texture enhancement. *Acta Materialia* **2012**, *60*, 4431–4437.

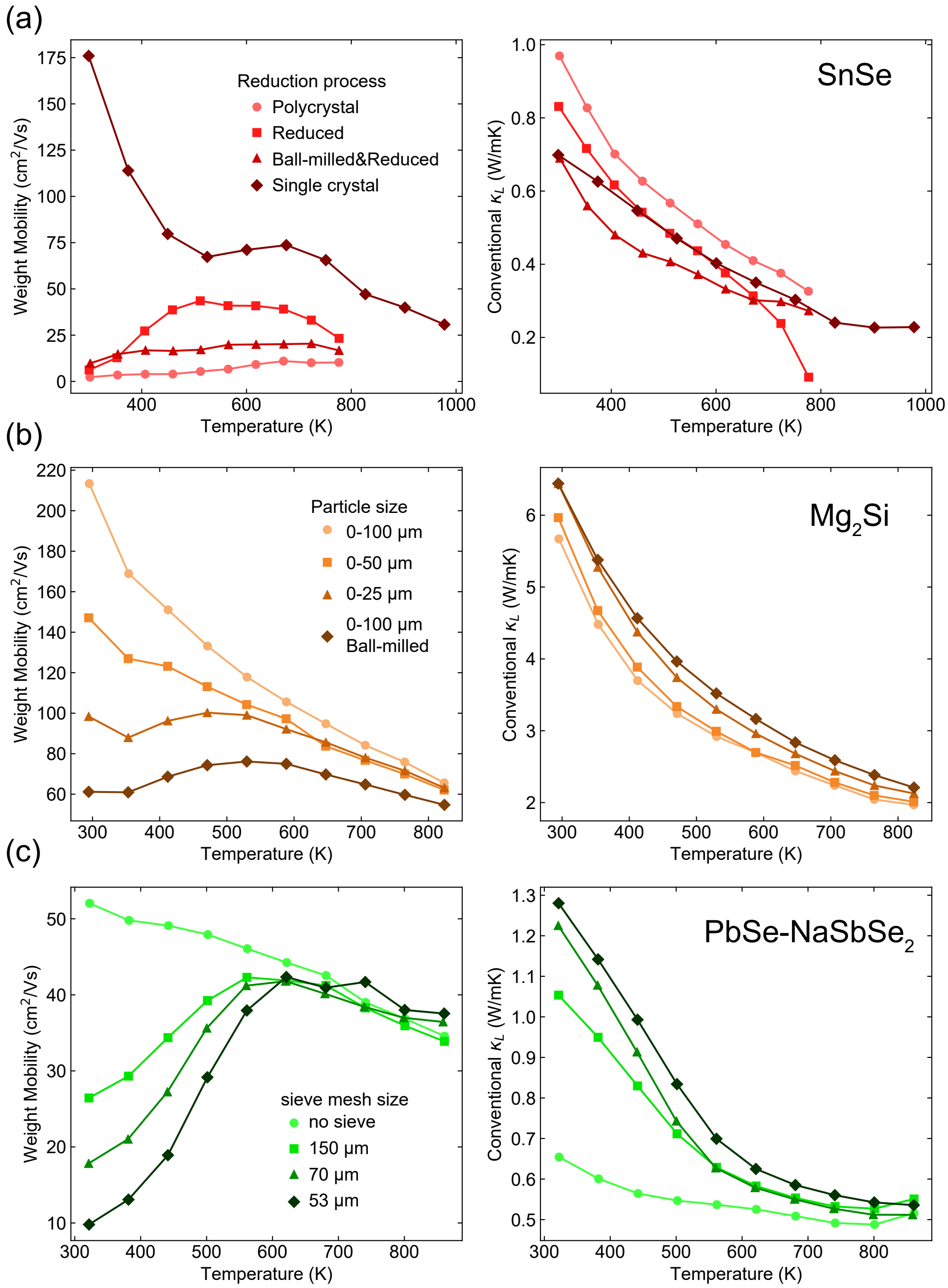

Figure S2: Weighted mobility and conventional lattice thermal conductivity of materials synthesized with different grain sizes (Mg_2Si,[6] PbSe alloy,[7,8] and SnSe[9,10]).

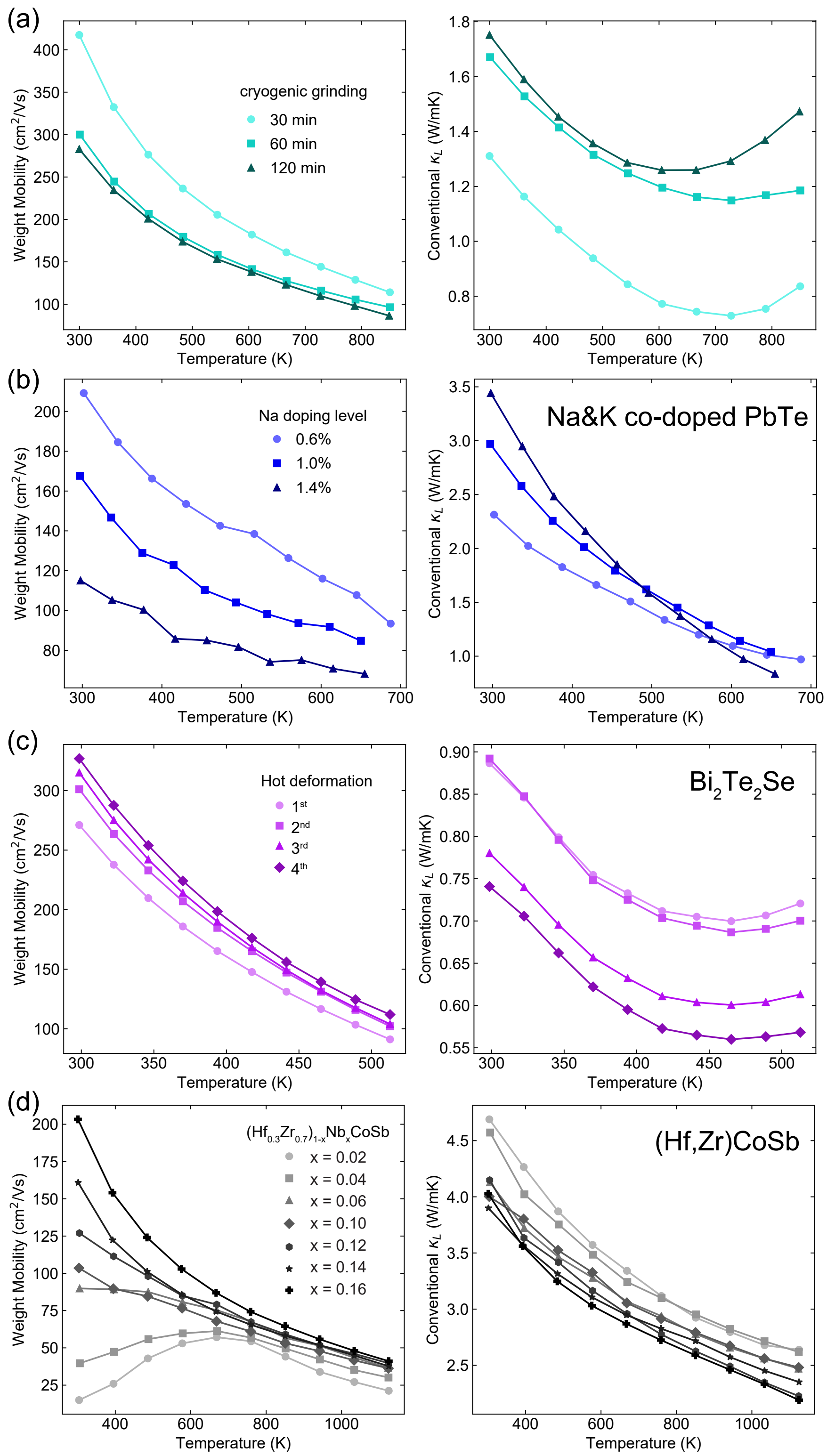

Figure S3: Weighted mobility and conventional lattice thermal conductivity of materials processed without specifically targeting their grain-boundary properties but showing a similar trend as Mg_3Sb_2 (PbTe, (Hf,Zr)CoSb,[11] $CoSb_3$,[12] and Bi_2Te_2Se[13]).